Atlas of spherical four-bar mechanisms

G. Mullineux[a,*]

[a] *Innovative Design and Manufacturing Research Centre, Department of Mechanical Engineering, University of Bath, Bath BA2 7AY, UK*

Abstract

An atlas or catalogue of mechanisms provides a useful aid in the synthesis of mechanisms for new applications. The atlas stores mechanisms together with their coupler paths. Fourier techniques can be used as a convenient means for representing, in normalized form, curves for planar mechanisms. This paper looks at the extension to spherical four-bar mechanisms. In particular, a means for projecting a spherical curve onto a plane is discussed which depends only on the geometry of the curve and not on the choice of world coordinate system.

Keywords: spherical mechanism, four-bar mechanism, mechanism synthesis, atlas, catalogue, Fourier series

1. Introduction

Mechanisms and, in particular spherical mechanisms, have a wide range of uses. These include function and motion generation, possibly between given precision points [1, 2] or to achieve given spatial re-orientations of an object [3]. Spherical mechanisms can be used as grippers [4] or wrists [5, 6] within robotic systems; and a recent extension of this is to robotic surgery [7, 8]. They have also been proposed as means of establishing orientations in aerospace [9] and of creating flapping wings for emulating natural flight [10, 11].

One area of design interest is that of mechanism synthesis. Here mechanisms which can potentially achieve a given task are sought. Many search

*Corresponding author

Email address: G.Mullineux@bath.ac.uk (G. Mullineux)

methods have been proposed to deal with the synthesis problem (for example [12, 13, 14, 15]). These use optimization techniques to change a given mechanism to one which more accurately generates a prescribed path, usually a coupler path.

The success of these approaches depends upon the mechanism selected to start the search process. One approach to obtaining a good start point is the use of some form of atlas or catalogue of mechanisms. Before easy access to computer systems was available, such atlases were provided in the form of printed books [16]. Today, computer-based atlases are possible. In use, the curve to be generated is specified. The atlas is then searched and the best ten or so mechanisms are made available [17]. This allows the designer some choice of which to use as the starting point for finding a more optimal solution and, if required, additional constraints on performance can be imposed [18, 19, 20, 21]. In setting up an atlas, some means of recording the properties of the coupler curve needs to be employed. Methods that have been investigated include the use of wavelets [22], and the purely geometric properties of the curve [23], in particular its curvature [24].

Much of the previous work on atlases has been concerned with planar mechanisms. There has however been recent interest in atlases for spherical mechanisms, in particular four-bar linkages [25, 26]. The approach used is to describe the coupler curve in terms of Fourier coefficients, an approach which works well for planar curves [27, 28]. The task is more difficult when the curve lies on a spherical surface. The solution previously adopted [25, 26] is to project the curve onto a plane perpendicular to the x-axis of the world coordinate system. The choice of a specific axis seems somewhat arbitrary (although any four-bar mechanism can be re-oriented so that the fixed pivot for the crank link lies on this axis). There appears also to be the possibility that some detail of the coupler curve may lost. This occurs, for example, if the curve is distant from the x-axis and so presents a projected profile which is roughly a circular arc rather than a closed curve.

The purpose of this paper is to present an alternative means of projection which takes account of the purely geometric properties of the curve and so does not depend on the particular orientation of the axes. This new approach is also different in that it fits the given curve to a sphere as a separate part of the process. This is useful as it provides a measure of how closely the curve lies on a sphere. Furthermore it can be used to normalize the curve so that it lies on a unit sphere centred at the origin. This helps during comparison with the curves generated by mechanisms in the atlas.

Section 2 reviews the use of Fourier coefficients for describing a planar curve. Geometric meaning can be assigned to the coefficients for low harmonics, and this allows curves to be normalized to remove the effects of differences due to scaling, translation and rotation. Section 3 gives an overview of the approach used here for creating and then using an atlas of spherical four-bar mechanisms. The procedure for projecting a closed curve onto a plane dependent upon its geometry is given in section 4, and the method for finding the best sphere fitting the given curve is given in section 5. Section 6 discusses how optimization techniques can be used to improve the match between a curve from the atlas and the required path. Section 7 provides an example of using an atlas to find spherical mechanisms to generate a given curve, and section 8 draws some conclusions.

2. Fourier representation

The use of Fourier coefficients to represent closed planar curves [28] is here briefly reviewed. For convenience, the curve is regarded as being made up of discrete points and these are taken to lie in the complex plane. This means that the typical point is a complex number of the form

$$z(t) = x(t) + iy(t)$$

where i is the square root of -1 and t is a parameter (which might for example represent time). For simplicity, it is assumed that the parameter is normalized to run between 0 and 1 as the curve is traced out, with $z(0) = z(1)$.

The standard Fourier theory (assuming that $z(t)$ satisfies Dirichlet's conditions [29]) says that $z(t)$ can be represented as the doubly infinite series

$$z(t) = \sum_{m=-\infty}^{\infty} c_m \exp(2\pi imt)$$

where the constant coefficients c_m are normally non-real and are given by

$$c_m = \int_0^1 \exp(-2\pi imt) z(t)\, dt \tag{1}$$

with the integral being over a full cycle.

For convenience, the coefficient c_0 is called the fundamental, coefficients c_1 and c_{-1} are regarded as forming the first harmonic, coefficients c_2 and c_{-2} the second harmonic, and so on.

It is unlikely, in practice, that a required output curve is available as an explicit function. It is often more convenient to describe the curve in terms of a sequence of points lying along it. This means that the integrations need to be carried out numerically. Suppose that N points are prescribed along the curve

$$z_0, z_1, z_2, \ldots, z_{N-1}$$

and this sequence is treated as being circular in the sense that z_{k+N} is the same point as z_k.

There are two cases that can be considered. Suppose that the points correspond to equally spaced values of the parameter t, which is regarded as representing the time taken in travelling along the curve. The step length for numerical integration is $(1/N)$. The trapezium rule gives the following approximation for the Fourier coefficients.

$$c_m \;=\; \frac{1}{N}\sum_{k=0}^{N-1} z_k \,\exp(-2\pi imk/N) \qquad (2)$$

This is the *time dependent* case. If some of the points are given close together, then progress around the curve is slowed down. If others are spaced out, then the speed is greater. The *time independent* case, in which the points simply represent the geometry of the path, can be dealt with similarly [28].

There are certain properties of the Fourier coefficients which can be drawn out. When $m = 0$, equation (1) states that the fundamental coefficient, c_0, is simply the average of all the points along the path. It thus represents their centroid. When dealing with a path defined by discrete points, equation (2) shows that this coefficient is the average of the given points.

This means that $z(t) - c_0$ is a closed curve whose centroid is at the origin of the complex plane.

The first harmonic terms form the function

$$z_1(t) \;=\; c_1 \exp(2\pi it) \;+\; c_{-1}\exp(-2\pi it)$$

which can be rewritten as

$$z_1(t) \;=\; \exp(i\alpha)[(r_1 + r_{-1})\cos(2\pi t + \beta) \;+\; i(r_1 - r_{-1})\sin(2\pi t + \beta)]$$

where

$$\begin{aligned} r_1 &= |c_1| \\ r_{-1} &= |c_{-1}| \\ \alpha &= [\arg(c_1) + \arg(c_{-1})]/2 \\ \beta &= [\arg(c_1) - \arg(c_{-1})]/2 \end{aligned}$$

In the expression for $z_1(t)$, the term in the square brackets generates an ellipse. Its centre is at the origin of the complex plane and its semi-major and semi-minor axes are of lengths (r_1+r_{-1}) and (r_1-r_{-1}) respectively. The ellipse is multiplied by the complex exponential $\exp(i\alpha)$ which has the effect of rotating it through an angle α anticlockwise.

If $r_1 > r_{-1}$, then the semi-major axis has positive length and this means that the ellipse is traced out anticlockwise as t varies from 0 to 1. If $r_1 < r_{-1}$, then the ellipse goes clockwise. If $r_1 = r_{-1}$, then the ellipse reduces to a straight line lying at angle α to the real axis.

The same idea also applies to the higher harmonics. The expression

$$z_m(t) \;=\; c_m \exp(2\pi imt) \;+\; c_{-m} \exp(-2\pi imt)$$

again represents an ellipse centred at the origin. However, as the parameter t goes from 0 to 1, this ellipse is traced out m times.

Figure 1 shows an example of building up a given closed curve from its harmonics. The main part of the figure shows the original curve itself. Part 1 shows the ellipse formed by c_0 and the first harmonic terms. In part 2, the second harmonic terms are added in, and so on, with part 5 giving the result of the partial sum of the Fourier series up to and including the fifth harmonic. It is seen that the original curve is reproduced accurately with just three harmonics (except for the sharp corner which is not well represented until higher harmonics are introduced). Table 1 gives the complex Fourier coefficients of the fundamental and first five harmonics. What is seen is that the (absolute) values of these decrease for the higher harmonics.

It is possible to use the Fourier coefficients to perform normalization on the curve [28]. As noted above, the centroid can be moved to the origin by translating through $-c_0$. For the new curve c_0 becomes zero. The coefficients for the first harmonic are next used. The curve is rotated through angle $-\alpha$ which tends to align the largest diameter across the curve with the real axis. This has the effect of multiplying the Fourier coefficients by $\exp(-i\alpha)$.

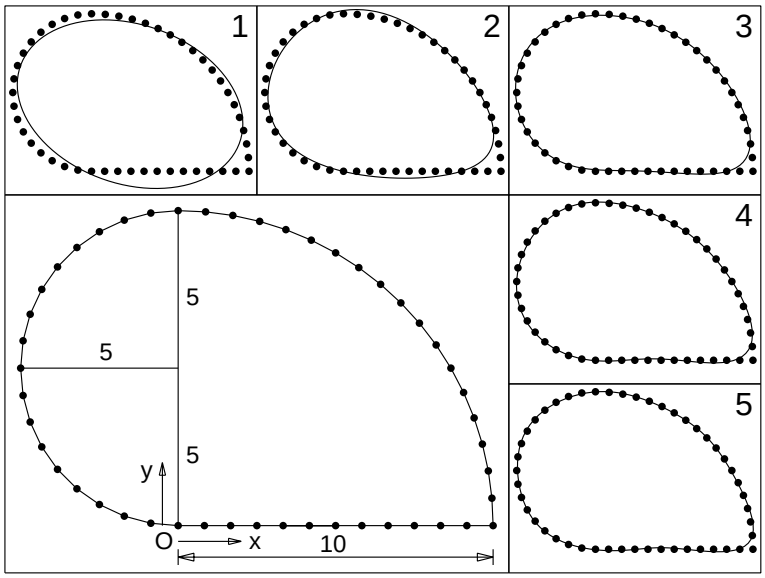

Figure 1: Approximations to a closed curve using partial sums of harmonics

If $|c_1| > |c_{-1}|$, then the curve is traced out in the anticlockwise sense. If this inequality does not hold, then all the c_m and c_{-m} are interchanged. The value of $|c_1|$ can be regarded as a scaling factor. The curve is further normalized by dividing all the Fourier coefficients by $|c_1|$.

The next step is to adjust the point of the curve where the parameter is zero. The normalization undertaken so far has reduced c_1 to $\exp(i\beta)$. If the parameter t is replaced as follows

$$t \;\mapsto\; t \,+\, \beta/2\pi$$

then the Fourier coefficient c_m becomes $c_m \exp(-i\beta)$. In particular, the coefficients for the first harmonic become purely real, with $c_1 = 1$ and $c_{-1} = r_{-1}$.

The final piece of normalization relates to the coefficient c_{-2} which is related to the second harmonic. Its real and imaginary parts are both made positive as follows. If its real part is negative, then the signs are reversed of the real parts of the even coefficients and the imaginary parts of the odd coefficients. This corresponds to a reflection in the imaginary axis (although it is more convenient to obtain it by a reflection in the real axis and incrementing α and β by π). If the imaginary part of c_{-2} is negative, then the signs of

m	c_m
-5	$-0.027 - 0.080i$
-4	$0.096 - 0.103i$
-3	$0.315 + 0.151i$
-2	$0.301 + 0.006i$
-1	$-2.875 - 5.511i$
0	$2.445 + 4.261i$
1	$0.212 + 1.138i$
2	$-0.336 + 0.157i$
3	$-0.120 - 0.097i$
4	$0.073 - 0.037i$
5	$0.029 + 0.071i$

Table 1: Fourier coefficients for closed path in figure 1

the imaginary parts of all the coefficients are reversed. This is equivalent to a reflection in the real axis.

These various normalization steps leave the curve and its Fourier parameters in a standard form. The overall normalization process represents a transformation of the plane. Of course, the original curve can be recovered by applying the inverse transform to the normalized points.

3. Approach

The typical spherical four-bar mechanism is shown in figure 2. It comprises three moving links: the crank AB, the coupler BC, and the driven link CD. The pivots A and D are fixed on a sphere. The sphere is assumed to have unit radius with its centre at the origin. The links can be regarded as arcs of great circles and their lengths are equal to the angles subtended at the centre of the sphere. Let $|DA| = a_0$, $|AB| = a_1$, $|BC| = a_2$, $|CD| = a_3$.

The point P is an offset point which moves with the coupler link BC. As the mechanism cycles, P traces out a coupler curve. The position of P can be specified in a number of ways. One way is shown in figure 3. This shows the coupler link (in its own local coordinate system) lying on a sphere with centre O with the link itself represented by the arc BC lying in the (local) xy-plane. End B lies on the x-axis. Plane OPF is perpendicular to plane OBC. The angles θ and ϕ shown in the figure then determine the position

of P. The lengths of the great arcs BP and CP are given as follows [30].

$$\begin{aligned} b_1 &= |BP| = \cos^{-1}[\cos(\phi)\cos(\theta)] \\ b_2 &= |CP| = \cos^{-1}[\cos(\phi)\cos(a_2 - \theta)] \end{aligned}$$

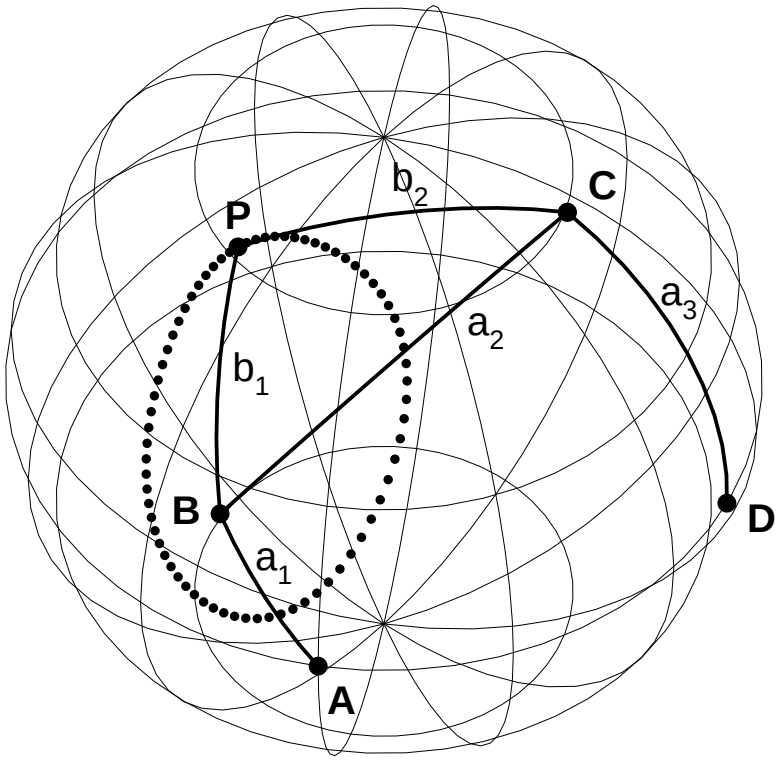

Figure 2: Notation for spherical four-bar mechanism

To construct an atlas of mechanisms, a means is required for obtaining a normalized form of the coupler curve for a given mechanism. An overview is given here and more details are added in later sections. In order to apply the Fourier technique of section 2, the coupler curve needs to be converted to a planar curve. A *central axis* is constructed (as discussed in section 4) which passes through the "middle" of the curve. This depends purely upon its geometry and is independent of the coordinate system used. Figure 4 shows a curve (part 1) and its central axis (part 2). It is straightforward to

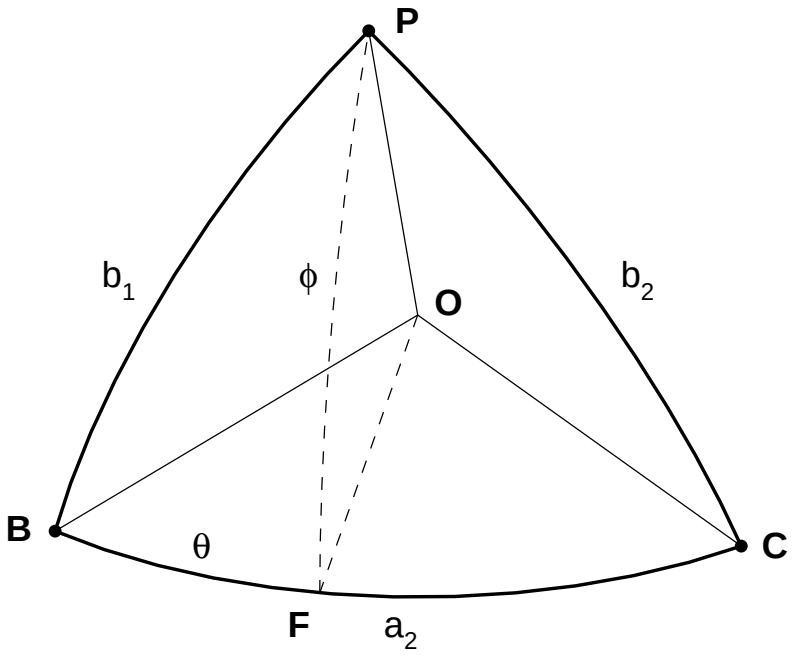

Figure 3: Notation for coupler link

find a rotation (about an axis through the origin) of the sphere which brings the central axis into the positive z-direction (part 3 of figure 4). The curve is now projected onto the xy-plane as shown in part 4 of the figure (cf. section 4).

The Fourier normalization is now applied to the planar curve. Importantly, no translation of the curve can be allowed as this would move it away from the sphere. So the central axis is chosen so that the centroid of the curve lies at the origin of the plane and no translation is needed. The normalizing transform requires a rotation of the curve (about the central axis) as shown in part 5 of figure 4. It may also require a scaling and a reflection as discussed in section 2.

The curve and the mechanism that creates it can now be added to the atlas. The mechanism parameters a_0, a_1, a_2, a_3, θ, ϕ are stored together with details of the normalizing transform and the first few Fourier coefficients of the curve. For the examples used here, the fundamental and the first five harmonics are used. Since the dyad formed by the coupler and driven links can assemble in either of two ways, it is also necessary to record which one is used. This can be done by storing, for one position in the cycle, the angular

orientations of the crank and driven links with respect to the base arc AD, and the orientation of the coupler with respect to the crank.

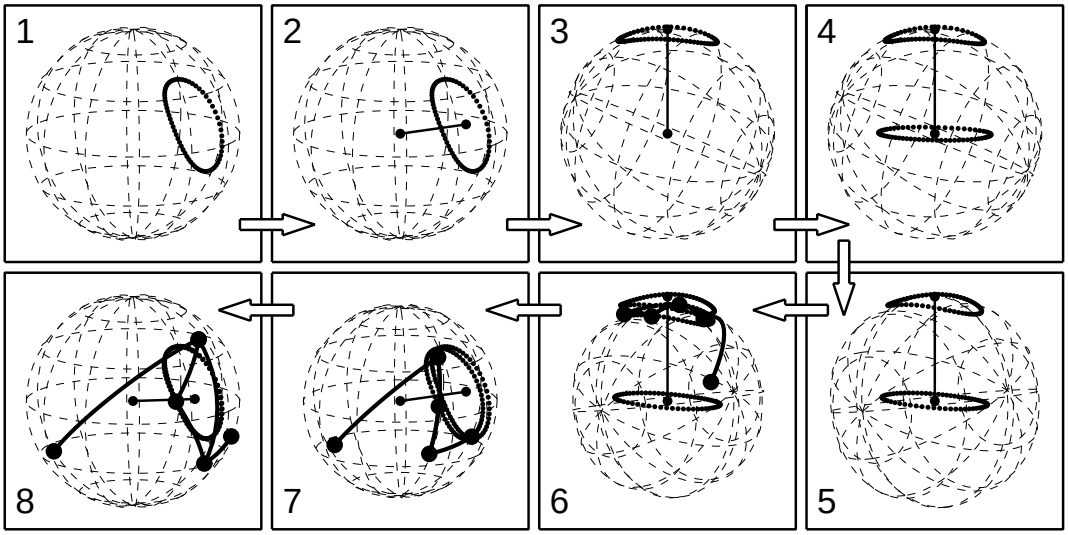

Figure 4: Normalizing a curve and unnormalizing a mechanism

The full atlas is created by building a parametric model of the spherical four-bar mechanism and then running this over combinations of variations in the values of the six parameters a_0, a_1, a_2, a_3, θ, ϕ. Since part of the normalization process is the rotation to bring the central axis into the z-direction, there is no need to consider variations in the positions of the pivots A and D. It is sufficient to take (say) A along the positive x-axis and for D to lie in the xy-plane.

When each variant mechanism is run, it is checked to see that it completes a full cycle and that the coupler curve returns to its start point. If these tests fail, then of course the mechanism is not entered into the atlas. Other tests for suitability can be applied: for instance, that the transmission angles between pairs of links lie in acceptable ranges.

When the atlas is used, the procedure is similar. A closed curve is specified. It assumed that this lies on (or close to) a sphere. The centre and radius of this sphere are found using a least squares technique (cf. section 5). The path is translated so that the centre of the sphere lies at the origin, and scaled so that the radius is unity.

The curve is then normalized by finding its central axis, rotating this into

the z-direction, projecting the curve onto the xy-plane, and applying the Fourier normalization (parts 1-5 of figure 4). Suppose that T_c is the overall transform applied to the curve.

The Fourier coefficients of the curve c_m are now found. These are now compared with the coefficients c'_m of each entry in the atlas. The measure of closeness is

$$\sum |c_m - c'_m|^2$$

(where the sum is for the first few harmonics that are used) and the entries with the lowest scores are extracted. Part 6 of figure 4 shows such a mechanism and the curve it generates. If T_e is the transform applied to the extracted mechanism when it was stored, then the transform $T_c^{-1}T_e$ is applied to the mechanism (in its original coordinate system) to obtain a mechanism generating approximately the given path (in its original coordinate system).

The purpose of the atlas is not to find a perfect match with a given curve, but instead to provide a starting point from which to search for a suitable mechanism. Optimization techniques can be applied to improve the match (part 8 of figure 4). Many methods are available for such optimization and their use is discussed in section 6.

As seen in parts 6 and 7 of figure 4, the approximating curve may not lie on a unit sphere because of the scaling applied when it was stored. So it is necessary during the optimization process, to reset this radius to unity.

It is of course possible, when the atlas is created, not to invoke the scaling part of the Fourier normalization so that the radius is always correct. However, allowing scaling to take place gives potentially a greater selection of possible approximations and, for this reason, scaling is used in the atlas here.

Rather than just finding the closest match in the atlas, it is also worth selecting the closest first few and presenting these to the user. It is likely these alternative mechanisms are different and some may be more acceptable (as starting points) than others in view of additional constraints that need to be taken into account, perhaps regarding positions of the pivots and avoidance of clashes.

4. Creating a planar curve

This section considers the projection of a closed curve on the surface of a sphere onto a plane. It is assumed that the sphere has unit radius and that

its centre lies at the origin O. If a point Q on the surface of the sphere is chosen, then a gnomonic or central projection [31] can be used, mapping the sphere onto the plane through Q perpendicular to the radial line OQ. Figure 5 shows the projection. If $\mathbf{r}$ is the position vector of a point on the sphere, then its image $\mathbf{R}$ is

$$\mathbf{R} \;=\; \left(\frac{1}{\mathbf{r}\cdot\mathbf{q}}\right)\mathbf{r}$$

where $\mathbf{q}$ is the position vector of Q relative to the origin. It is radial line OQ that is used as the *central axis* in the approach given in section 3. Care in the choice of Q is needed as is now discussed.

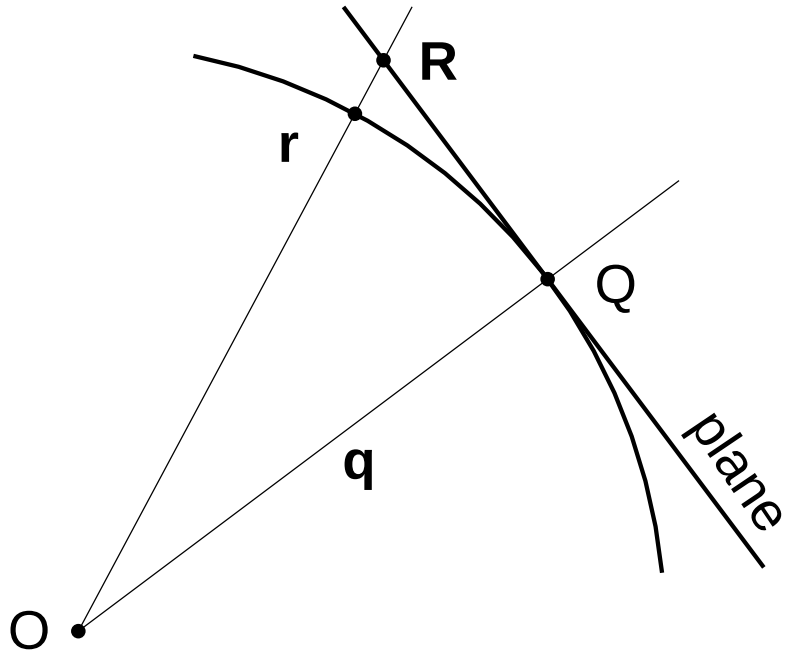

Figure 5: Gnomonic projection

Suppose that the given curve on the sphere is $\mathbf{r}(s)$ where s represents arc length along that curve. Then for the corresponding projected curve $\mathbf{R}(s)$,

$$\frac{\mathrm{d}\mathbf{R}}{\mathrm{d}s} \;=\; \frac{1}{(\mathbf{r}\cdot\mathbf{q})^2}\left[(\mathbf{r}\cdot\mathbf{q})\mathbf{r}' \;-\; (\mathbf{r}'\cdot\mathbf{q})\mathbf{r}\right]$$

where the dash denotes differentiation with respect to s. Using the facts that $\mathbf{r} \cdot \mathbf{r} = 1 = \mathbf{r}' \cdot \mathbf{r}'$ and $\mathbf{r} \cdot \mathbf{r}' = 0$, it follows that

$$(\mathbf{r} \cdot \mathbf{q})^4 \, \mathbf{R}' \cdot \mathbf{R}' \;=\; (\mathbf{r} \cdot \mathbf{q})^2 \;+\; (\mathbf{r}' \cdot \mathbf{q})^2$$

Let S denote arc length along the projected curve. Then $|\mathbf{R}'| = \mathrm{d}S/\mathrm{d}s$, and hence

$$\frac{\mathrm{d}S}{\mathrm{d}s} \;=\; \frac{1}{(\mathbf{r} \cdot \mathbf{q})^2} \left[(\mathbf{r} \cdot \mathbf{q})^2 \;+\; (\mathbf{r}' \cdot \mathbf{q})^2 \right]^{\frac{1}{2}}$$

The projection used needs to ensure that the Fourier coefficient c_0 of the projected curve is zero, so that no translation is required in its normalization (cf. section 2). Since c_0 represents the centroid of the curve by equation (1), consider $\mathbf{C}$ the position vector of centroid of the projected curve relative to Q. If L is the total length of the projected curve, then

$$L\mathbf{C} \;=\; \int [\mathbf{R}(s) - \mathbf{q}] \, \mathrm{d}S \;=\; \left(\int \mathbf{R}(s) \, \mathrm{d}S \right) \;-\; L\mathbf{q}$$

and

$$\begin{aligned} L(\mathbf{q} + \mathbf{C}) \;&=\; \int \mathbf{R}(s) \, \frac{\mathrm{d}S}{\mathrm{d}s} \, \mathrm{d}s \\ &=\; \int \frac{1}{(\mathbf{r} \cdot \mathbf{q})^3} \left[(\mathbf{r} \cdot \mathbf{q})^2 \;+\; (\mathbf{r}' \cdot \mathbf{q})^2 \right]^{\frac{1}{2}} \mathbf{r} \, \mathrm{d}s \end{aligned} \tag{3}$$

The requirement that $\mathbf{C} = \mathbf{0}$ leads to the following eigen-problem whose solution is $\mathbf{q}$.

$$L\mathbf{q} \;=\; \int \frac{1}{(\mathbf{r} \cdot \mathbf{q})^3} \left[(\mathbf{r} \cdot \mathbf{q})^2 \;+\; (\mathbf{r}' \cdot \mathbf{q})^2 \right]^{\frac{1}{2}} \mathbf{r} \, \mathrm{d}s \tag{4}$$

It is possible to solve equation (4) directly by numerical methods. An alternative is to minimize the right hand side of equation (3) with respect to variation in the unit vector $\mathbf{q}$.

However, as the atlas is only intended to provide starting points for mechanism searches, great accuracy in the choice of $\mathbf{q}$ is not necessary. So consider the following approximation. Assume that the curve is "small" and lies close

to the point Q. Then for all points $\mathbf{r}(s)$ on the given curve, $\mathbf{r} \cdot \mathbf{q} \simeq 1$ and $\mathbf{r}' \cdot \mathbf{q} \simeq 0$. Equation (4) now becomes

$$L\mathbf{q} \;=\; \int \mathbf{r}(s)\,\mathrm{d}s \tag{5}$$

Thus the vector $\mathbf{q}$ can be found by evaluating the integral in equation (5), and this only involves the given curve.

If the curve is specified as a sequence of N discrete points $\mathbf{r}_i$ for $0 \leq i \leq N-1$, then the integral can be evaluated using the trapezium rule. This leads to the following expression for $\mathbf{q}$

$$\mathbf{q} \;=\; \lambda \sum_{i=0}^{N-1} \tfrac{1}{2}\,(\mathbf{r}_{i+1} + \mathbf{r}_i)\,|\mathbf{r}_{i+1} - \mathbf{r}_i| \tag{6}$$

where the sequence is regarded as being circular, so that $\mathbf{r}_N = \mathbf{r}_0$, and λ is the scalar factor required to make $\mathbf{q}$ a unit vector. This provides the central axis OQ for normalizing the given curve.

5. Spherical fitting

It is necessary to consider how to find a best fit sphere through a given collection of 3D points. Suppose that n points are given with coordinates (x_i, y_i, z_i) for $1 \leq i \leq n$. If the best fit sphere through these points has radius R and centre at (X, Y, Z), then its equation is

$$(x - X)^2 \;+\; (y - Y)^2 \;+\; (z - Z)^2 \;-\; R^2 \;=\; 0$$

So a measure e_i of the error at point i is

$$e_i \;=\; r_i^2 \;-\; 2Xx_i \;-\; 2Yy_i \;-\; 2Zz_i \;-\; K$$

where

$$r_i^2 \;=\; x_i^2 \;+\; y_i^2 \;+\; z_i^2$$

and

$$K \;=\; R^2 \;-\; X^2 \;-\; Y^2 \;-\; Z^2$$

Then the total error E can be measured as

$$E \;=\; \sum_{i=0}^{n} e_i^2 \;=\; \sum_{i=0}^{n} [r_i^2 - 2Xx_i - 2Yy_i - 2Zz_i - K]^2$$

Following the usual least squares approach, E is treated as a function of X, Y, Z and K. When E is minimal, its partial derivatives are zero.

$$\begin{aligned}
\frac{\partial E}{\partial X} &= -4\sum_{i=0}^{n}[r_i^2 - 2Xx_i - 2Yy_i - 2Zz_i - K]x_i \;=\; 0 \\
\frac{\partial E}{\partial Y} &= -4\sum_{i=0}^{n}[r_i^2 - 2Xx_i - 2Yy_i - 2Zz_i - K]y_i \;=\; 0 \\
\frac{\partial E}{\partial Z} &= -4\sum_{i=0}^{n}[r_i^2 - 2Xx_i - 2Yy_i - 2Zz_i - K]z_i \;=\; 0 \\
\frac{\partial E}{\partial K} &= -2\sum_{i=0}^{n}[r_i^2 - 2Xx_i - 2Yy_i - 2Zz_i - K] \;=\; 0
\end{aligned}$$

These represent a system of linear equations for finding the four unknowns. The system can be rewritten in matrix form

$$\begin{bmatrix}
\sum_{i=1}^{n} x_i^2 & \sum_{i=1}^{n} x_i y_i & \sum_{i=1}^{n} x_i z_i & \sum_{i=1}^{n} x_i \\
\sum_{i=1}^{n} x_i y_i & \sum_{i=1}^{n} y_i^2 & \sum_{i=1}^{n} y_i z_i & \sum_{i=1}^{n} y_i \\
\sum_{i=1}^{n} x_i z_i & \sum_{i=1}^{n} y_i z_i & \sum_{i=1}^{n} z_i^2 & \sum_{i=1}^{n} z_i \\
\sum_{i=1}^{n} x_i & \sum_{i=1}^{n} y_i & \sum_{i=1}^{n} z_i & \sum_{i=1}^{n} 1
\end{bmatrix}
\begin{bmatrix} 2X \\ 2Y \\ 2Z \\ K \end{bmatrix}
=
\begin{bmatrix}
\sum_{i=1}^{n} r_i^2 x_i \\
\sum_{i=1}^{n} r_i^2 y_i \\
\sum_{i=1}^{n} r_i^2 z_i \\
\sum_{i=1}^{n} r_i^2
\end{bmatrix} \qquad (7)$$

where $\sum_{i=1}^{n} 1 = n$, the number of points.

As an example, consider the set of 64 points around the 3D path given in Table 3 of [25]. Setting up and solving equation (7) yields: $X = 10$, $Y = -5$,

$Z = -6$, and $R = 2.7$. Furthermore, evaluation of the error at each point shows that they lie exactly on this sphere (at least to the accuracy with which the points themselves are given). So the proposed path can be "normalized" by translating the centre of the sphere to the origin and then applying a scale factor of $1/R$ to create a unit sphere. Table 2 gives the resultant points and they are also shown in figure 6.

1	(0.85737, -0.18481, 0.48037)	33	(0.7887, -0.60370, 0.11578)
2	(0.82985, -0.20167, 0.52030)	34	(0.80152, -0.59270, 0.07900)
3	(0.80241, -0.21996, 0.55478)	35	(0.81378, -0.57959, 0.04311)
4	(0.77567, -0.23967, 0.58389)	36	(0.82552, -0.56433, 0.00841)
5	(0.75011, -0.26056, 0.60785)	37	(0.83678, -0.54700, -0.02478)
6	(0.72607, -0.28244, 0.62693)	38	(0.84759, -0.52763, -0.05611)
7	(0.70381, -0.30515, 0.64152)	39	(0.85807, -0.50641, -0.08530)
8	(0.68352, -0.32833, 0.65193)	40	(0.86819, -0.48344, -0.11200)
9	(0.66533, -0.35185, 0.65844)	41	(0.87804, -0.45889, -0.13596)
10	(0.64933, -0.37537, 0.66144)	42	(0.88763, -0.43304, -0.15689)
11	(0.63559, -0.39867, 0.66115)	43	(0.89704, -0.40611, -0.17448)
12	(0.62415, -0.42159, 0.65781)	44	(0.90626, -0.37837, -0.18848)
13	(0.61504, -0.44389, 0.65167)	45	(0.91537, -0.35022, -0.19867)
14	(0.60833, -0.46541, 0.64293)	46	(0.92433, -0.32193, -0.20481)
15	(0.60396, -0.48596, 0.63170)	47	(0.93322, -0.29396, -0.20667)
16	(0.60196, -0.50548, 0.61819)	48	(0.94196, -0.26667, -0.20400)
17	(0.60230, -0.52381, 0.60241)	49	(0.95052, -0.24048, -0.19667)
18	(0.60485, -0.54085, 0.58448)	50	(0.95885, -0.21581, -0.18441)
19	(0.60959, -0.55656, 0.56448)	51	(0.96685, -0.19315, -0.16707)
20	(0.61637, -0.57081, 0.54244)	52	(0.97430, -0.17289, -0.14452)
21	(0.62500, -0.58363, 0.51844)	53	(0.98096, -0.15541, -0.11656)
22	(0.63530, -0.59489, 0.49248)	54	(0.98652, -0.14104, -0.08315)
23	(0.64700, -0.60456, 0.46467)	55	(0.99052, -0.13007, -0.04430)
24	(0.65989, -0.61259, 0.43507)	56	(0.99244, -0.12263, -0.00019)
25	(0.67370, -0.61896, 0.40378)	57	(0.99174, -0.11870, 0.04874)
26	(0.68811, -0.62363, 0.37093)	58	(0.98774, -0.11822, 0.10185)
27	(0.70293, -0.62652, 0.33674)	59	(0.98000, -0.12085, 0.15807)
28	(0.71789, -0.62759, 0.30133)	60	(0.96819, -0.12626, 0.21604)
29	(0.73274, -0.62678, 0.26500)	61	(0.95226, -0.13415, 0.27426)
30	(0.74737, -0.62404, 0.22800)	62	(0.93252, -0.14411, 0.33115)
31	(0.76167, -0.61933, 0.19059)	63	(0.90956, -0.15600, 0.38515)
32	(0.77544, -0.61256, 0.15307)	64	(0.88422, -0.16959, 0.43519)

Table 2: Points around 3D path from [25] normalized to lie on unit sphere

6. Improving the match

The interest of this paper is in how to obtain mechanisms which are close to what is required by a design task so that they can be used as starting points for seeking better design solutions. However, simply to illustrate what can be done, this section briefly reviews the use of optimization techniques to

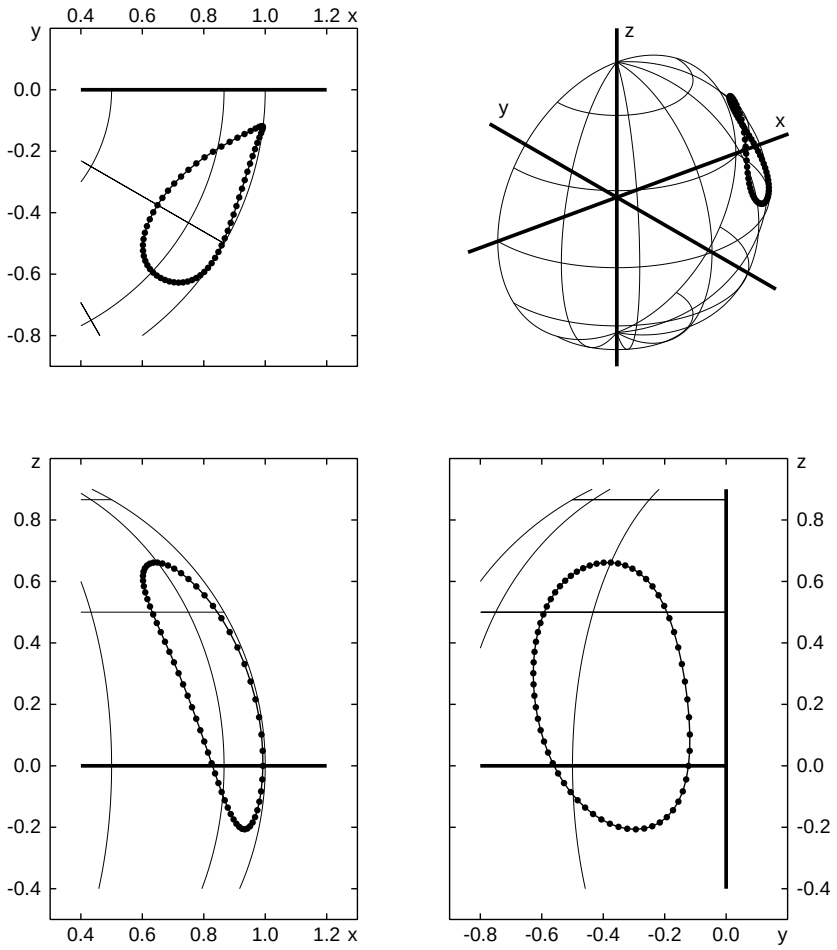

Figure 6: Views of points around 3D path from [25] normalized to lie on unit sphere

improve the match between the path that is obtained by the selection from the atlas and what is required. The improvement step is that suggested in part 8 of figure 4.

A number of methods for undertaking such improvement have appeared in the literature (for example [12, 13, 14, 15]). These use various optimization schemes to try to improve a suitable measure of the goodness of fit between the path generated by a candidate mechanism and given precision points.

It might be argued that such methods are over-elaborate when the mechanism is as simple as a spherical four bar linkage. The number of design variables is just nine: six are the parameters of the mechanism, and three

are those associated with a general rotation (about an axis through the centre of a the sphere). This means that any of the standard optimization methods (cf. [32]) is usable provided a good "seed" mechanism is available to start the search (and this is what the atlas provides). In particular, direct search methods are attractive as they do not require (explicit) information about derivatives.

The measure of fit can be a comparison of Fourier coefficients. Effectively this is an extension of the approach used to make the selection from the atlas. An alternative measure is the root mean square (rms) of the distances between corresponding points on the given and approximating curves.

It is this second measure that is used with the example in section 7. It has the advantage that it deals with the actual geometry of the situation and so reduces dependency on the assumptions made using the Fourier representation. These include the use of a limited number of Fourier coefficients and the approximation inherent in regarding the curve as being small (section 4). (Such assumptions are of course of no consequence when the atlas is used to select a mechanism as the aim then is simply to find a close approximate match.) The other reason for the choice of measure is that in the implementation used to deal with the examples here, the final improvement stage was undertaken separately from the use of the atlas. It was carried out using a constraint modelling environment (discussed in [33]) and it was more straightforward to evaluate the rms measure in the user language of that environment. The optimization method used (within the environment) was Powell's direct search method [32] (but other methods work as well).

7. Example of using the atlas

An example is given of using an atlas to find spherical four-bar mechanisms which can generate a given curve. The atlas is constructed as discussed in section 3. For simplicity, the atlas used here is created fairly coarsely with the variations in the values of the links lengths being 15 degrees. It is of course straightforward to create a more refined version at the expense of a larger size.

The example uses the same curve as given in [25]. It is specified by 64 points. The first stage here is to find a sphere upon which the points lie. This is done in section 5 and it allows the curve to be translated and scaled so that it lies on a unit sphere whose centre is at the origin. The resultant points are given in table 2.

The central axis is found using equation (6) and $\mathbf{q}$ is the vector with components $(0.8836, -0.3920, 0.2560)$. When the Fourier coefficients of the projected planar curve are found, the fundamental is $c_0 = (8 + 95i) \times 10^{-6}$, which is small and so shows that the approximation inherent in equation (5) is justified in this case.

The planar curve is used as the basis of a search of the atlas. Table 3 gives three selections, and these are shown in figures 7, 8 and 9. In the lower part of the table, R is the radius of the sphere, and A_x, A_y, A_z, D_x, D_y, D_z are the coordinates of the pivot points A and D. Mechanism 1 is the best match found in the atlas. Mechanism 2 is the next closest match. Mechanism 3 is a somewhat poorer match but is chosen here for illustration since its radius is significantly different from unity.

Also shown in the table is the result of improving each of the mechanisms by varying their link sizes (a_0, a_1, a_2, a_3, θ, ϕ) and orientations (nine degrees of freedom in total) and minimizing the root mean square (rms) of the distances between corresponding points on the given and approximate curves. As noted in section 6, Powell's direct search method was used for this improvement stage. Before the improvement, the rms values are not small (partly because the mechanisms have a radius other than unity), but after improvement, the values drop to less than 0.02.

As is clear, the original mechanisms from the the atlas and their improved versions are very dissimilar. This is a case where offering the designer more than one option from the atlas is helpful as it can allow other design considerations to be taken into account.

8. Conclusions

When creating an atlas of mechanisms and their coupler curves, a method is required to describe the curve and to normalize it (and its mechanism) so that duplicates are not stored and the size of the atlas is reduced. The use of Fourier coefficients is one way to achieve this for planar curves, and this allows normalization to remove the effects of translation, rotation and scaling.

This paper has considered the case of spherical four-bar mechanisms: here the coupler path is no longer planar. It has been seen that it is possible to find a sphere which is the best fit to a given curve and this allows the curve to be normalized (by translation and scaling) so that it lies on a unit sphere whose centre is at the origin.

	1 atlas	1 imp'd	2 atlas	2 imp'd	3 atlas	3 imp'd
a_0	90.00	63.22	90.00	50.80	60.00	88.38
a_1	90.00	24.88	30.00	25.71	15.00	26.26
a_2	90.00	65.07	60.00	42.63	60.00	39.94
a_3	90.00	55.64	75.00	35.83	75.00	99.05
θ	30.00	31.17	30.00	15.50	30.00	18.11
ϕ	0.00	29.32	0.00	15.33	-30.00	-4.90
b_1	30.00	41.75	30.00	21.67	41.41	18.74
b_2	30.00	43.64	30.00	30.88	41.41	22.35
R	0.9075	1.0000	0.9055	1.0000	1.6090	1.0000
A_x	0.8550	0.9704	0.5166	0.7383	1.0209	0.7615
A_y	-0.2175	0.1120	-0.4532	-0.3314	0.0013	-0.3613
A_z	-0.2130	-0.2140	0.5897	0.5874	1.2437	0.5382
D_x	0.2786	0.4511	0.4412	0.8323	0.2994	0.1093
D_y	0.8149	0.8139	0.7647	0.4695	1.3673	0.8696
D_z	0.2862	0.3661	0.2013	0.2947	0.7936	0.4816
rms	0.1115	0.0090	0.1180	0.0157	0.6359	0.0170

Table 3: Three mechanisms selected from atlas and their improved versions

It has also been shown how to construct a central axis, dependent only upon the geometry of the curve, so that the curve can be projected onto a plane normal to this axis, independent of the world coordinate system. This allows the Fourier technique to be used on the resultant planar curve which provides further normalization of the curve (by rotation and scaling).

An atlas of spherical four-bar mechanisms has been created using these techniques and its application to finding mechanisms to generate a given curve has been demonstrated.

The atlas deals with path of the coupler point and matching this with a design requirement. Spherical mechanisms have the property of generating motions within three dimensional space. So there may be a need not only to follow a given path but also to achieve a given orientation (of the local reference frame) at each step: thus it is the full motion that needs to be matched. Future work is to consider how to hold both position and orientation within the atlas (possibly in Fourier form), and then how to extract good matches to meet given motion requirements. A difficulty here is the fact that posi-

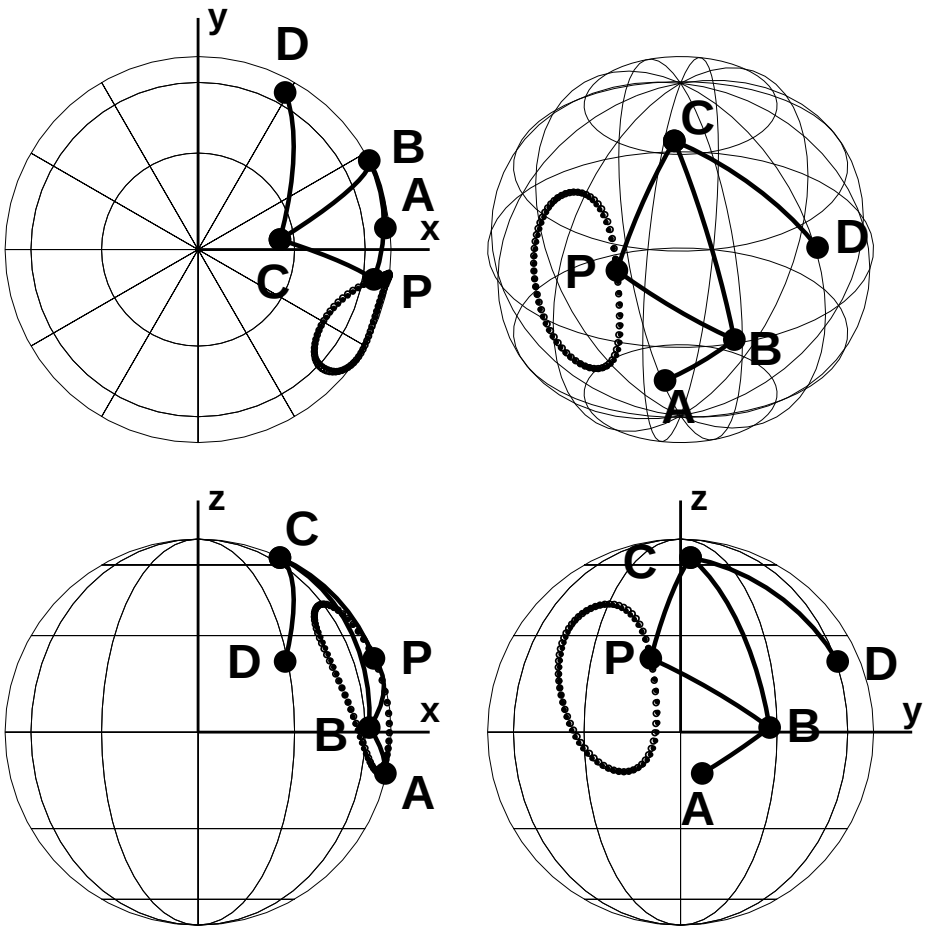

Figure 7: Improved version of mechanism 1 from atlas

tion and orientation are inherently not comparable. For example, position involves units of length, whereas an orientation angle is dimensionless.

Acknowledgements

The work reported in the paper was carried within the Innovative Design and Manufacturing Research Centre at the University of Bath. This is funded by the Engineering and Physical Sciences Research Council (EPSRC). The work relates to a project on reconfigurable packaging systems sponsored by the Department of the Environment, Food and Rural Affairs (DEFRA). This support is gratefully acknowledged.

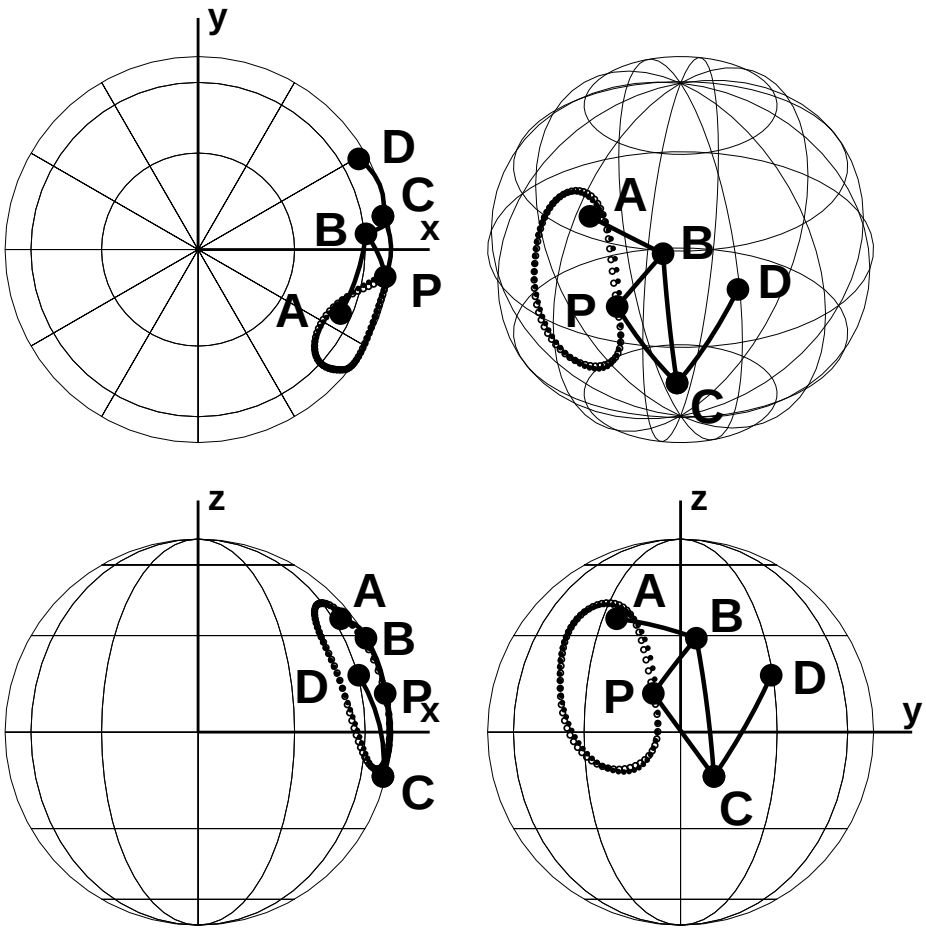

Figure 8: Improved version of mechanism 2 from atlas

References

[1] W.-T. Lee, K. Russell, Q. Shen, R.S. Sodhi, On adjustable spherical four-bar motion generation for expanded prescribed positions. Mechanism and Machine Theory 44 (2009) 247–254.

[2] Y. Suixan, Y. Hong, G.Y. Tian, Optimal selection of precision points for function synthesis of spherical 4R linkage. Proc. Instn Mech. Engrs, Part C: Journal of Mechanical Engineering Science 223 (2009) 2183–2189.

[3] A.P. Murray, F. Pierrot, Design of high-speed spherical four-bar mechanism for use in a motion common in assembly processes. Proc. ASME

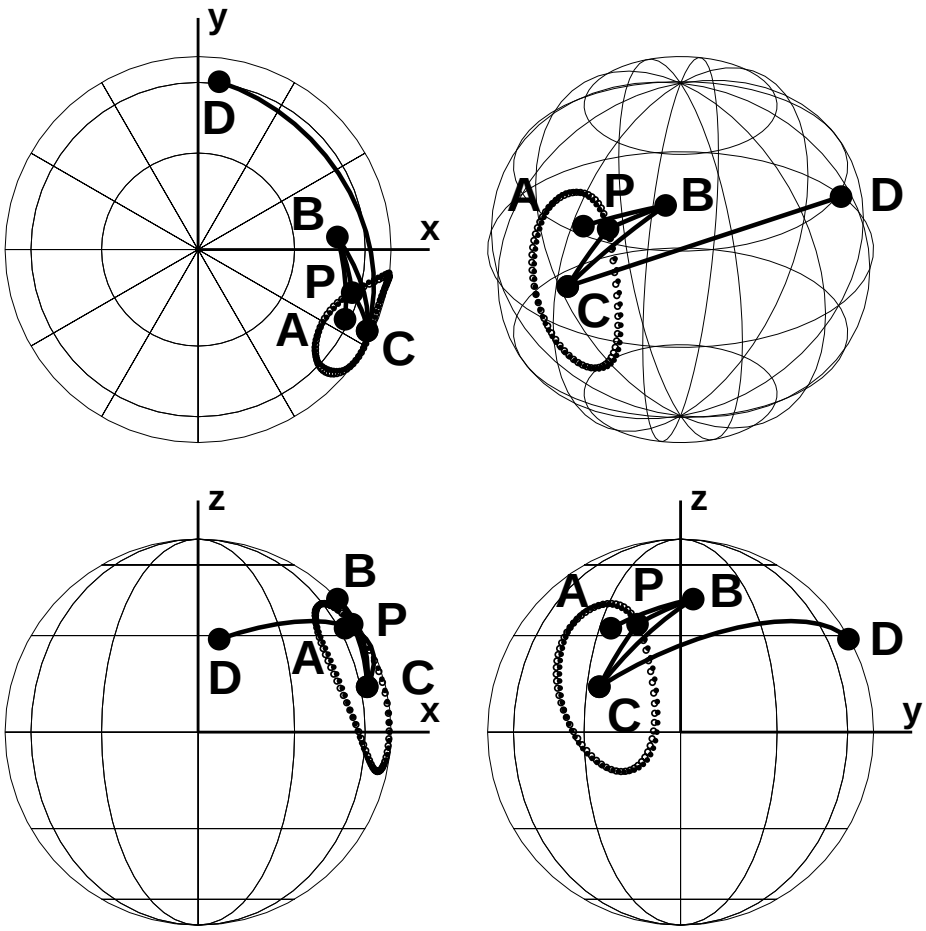

Figure 9: Improved version of mechanism 3 from atlas

International Design Engineering Technical Conferences and Computers and Information in Engineering Conference 2007 Volume 8 (2008) 511–518.

[4] H. Kocabas, Gripper design with spherical parallelogram mechanism. Journal of Mechanical Design 131 (2009) 075001:1–9.

[5] T.A. Hess-Coelho, A redundant parallel spherical mechanism for robotic wrist application. Journal of Mechanical Design 129 (2007) 891–895.

[6] D. Chablat, J. Angeles, The computation of all 4R serial spherical wrists

with an isotropic architecture. Journal of Mechanical Design 125 (2003) 275–280.

[7] A.C. Lehman, M.M. Tiwari, B.C. Shah, S.M. Farritor, C.A. Nelson, D. Oleynikov, Recent advances in the CoBRASurge robotic manipulator and dexterous miniature *in vivo* robotics for minimally invasive surgery. Proc. Instn Mech. Engrs, Part C: Journal of Mechanical Engineering Science 224 (2010) 1487–1494.

[8] M.J.H. Lum, J. Rosen, M.N. Sinanan, B. Hannaford, Optimization of a spherical mechanism for a minimally invasive surgical robot: theoretical and experimental approaches. IEEE Transactions on Biomedical Engineering 53 (2006) 1440–1445.

[9] C. Menon, R. Vertechy, M.C. Markót, V. Parenti-Castelli, Geometrical optimization of parallel mechanisms based on natural frequency evaluation: application to a spherical mechanism for future space applications. IEEE Transactions on Robotics 25 (2009) 12–23.

[10] M. McDonald, S.K. Agrawal, Design of a bio-inspired spherical four-bar mechanism for flapping-wing micro air-vehicle applications. Journal of Mechanisms and Robotics 2 (2010) 021012:1–6.

[11] Q.V. Nguyen, H.C. Park, N.S. Goo, D. Byun, Characteristics of a beetle's free flight and a flapping-wing system that mimics beetle flight. Journal of Bionic Engineering 7 (2010) 77–86.

[12] X. Zhang, C.A. Nelson, Multiple-criteria kinematic optimization for the design of spherical serial mechanisms using genetic algorithms. Journal of Mechanical Design 133 (2011) 011005:1–11.

[13] W.Y. Lin, S.S. Wang, Dimensional synthesis of a five-point double-toggle mould clamping mechanism using a genetic algorithm-differential evolution hybrid algorithm. Proc. Instn Mech. Engrs, Part C: Journal of Mechanical Engineering Science 224 (2010) 1305–1313.

[14] M.A. Laribi, A. Mlika, L. Romdhane, S. Zeghloul, A combined genetic algorithm-fuzzy logic method (GA-FL) in mechanisms synthesis. Mechanism and Machine Theory 39 (2004) 717–735.

[15] A. Vasiliu, B. Yannou, Dimensional synthesis of planar mechanisms using neural networks: application to path generator linkages. Mechanism and Machine Theory 36 (2001) 313–328.

[16] J.A. Hrones, G.L. Nelson, Analysis of the Four-Bar Linkage, Wiley, 1951.

[17] B. Singh, J. Matthews, G. Mullineux, A.J. Medland, Design catalogues for mechanism selection, in: D. Marjanović, M. Štorga, N. Pavković, N. Bojčretić (eds.), 10th International Design Conference DESIGN 2008, University of Zagreb, Croatia, 2008, 673–680.

[18] S. Erkaya, I. Uzmay, Determining link parameters using genetic algorithm in mechanisms with joint clearance. Mechanism and Machine Theory 44 (2009) 222–234.

[19] C.-M. Lee, V.N. Goverdovskiy, Type synthesis of function-generating mechanisms for seat suspensions. International Journal of Automotive Technology 10 (2009) 37–48.

[20] R. Rayner, M.N. Sahinkaya, B.J. Hicks, Combining inverse dynamics with traditional mechanism synthesis to improve the performance of high speed machinery, in: Proc. ASME 2008 Dynamic Systems and Control Conference (DSCC2008), Ann Arbor, 2008, 599–606.

[21] J.A. Cabrera, F. Nadal, J.P. Muñoz, A. Simon, Multiobjective constrained optimal synthesis of planar mechanisms using a new evolutionary algorithm. Mechanism and Machine Theory 42 (2007) 791–806.

[22] G. Galan-Martin, F.J. Alonso, J.M. Del Castillo, Shape optimization for path synthesis of crank-rocker mechanisms using a wavelet-based neural network. Mechanism and Machine Theory 44 (2009) 1132–1143.

[23] J. Buskiewicz, Use of shape invariants in optimal synthesis of geared five-bar linkage. Mechanism and Machine Theory 45 (2010) 273–290.

[24] J. Buskiewicz, R. Starosta, T. Walczak, On the application of the curve curvature in path synthesis. Mechanism and Machine Theory 44 (2009) 1223-1239.

[25] J.K. Chu, J.W. Sun, Numerical atlas method for path generation of spherical four-bar mechanism. Mechanism and Machine Theory 45 (2010) 867–879.

[26] J.W. Sun, J.K. Chu, Fourier series representation of the coupler curves of spatial linkages. Applied Mathematical Modelling 34 (2010) 1396–1403.

[27] R. Starosta, Application of genetic algorithm and Fourier coefficients (GA-FC) in mechanism synthesis. Journal of Theoretical and Applied Mechanics 46 (2008) 395–411.

[28] J.R. McGarva, G. Mullineux, Harmonic representation of closed curves. Applied Mathematical Modelling 17 (1993) 213–218.

[29] W. Bolton, Fourier Series, Longman, 1995.

[30] R. Fenn, Geometry, Springer-Verlag, London, 2001.

[31] H.S.M. Coxeter, Introduction to Geometry, 2nd edition, Wiley, New York, 1989.

[32] R. Fletcher, Practical Methods of Optimization, 2nd edition, Wiley, Chichester, 1987.

[33] G. Mullineux, J. Feldman, J. Matthews, Using constraints at the conceptual stage of the design of carton erection. Mechanism and Machine Theory 45 (2010) 1897–1908.